# Discovery of Antitubulin Agents with Antiangiogenic Activity as Single Entities with Multitarget Chemotherapy Potential

Aleem Gangjee,[†,*] Roheeth Kumar Pavana,[†] Michael A. Ihnat,[‡] Jessica E. Thorpe,[‡] Bryan C. Disch,[‡] Anja Bastian,[‡] Lora C. Bailey-Downs,[‡] Ernest Hamel,[§] and Rouli Bai[§]

[†]Division of Medicinal Chemistry, Graduate School of Pharmaceutical Sciences, Duquesne University, Pittsburgh, Pennsylvania 15282, United States

[‡]Department of Pharmaceutical Sciences, University of Oklahoma College of Pharmacy, Oklahoma City, Oklahoma 73117, United States

[§]Screening Technologies Branch, Developmental Therapeutics Program, Division of Cancer Treatment and Diagnosis, Frederick National Laboratory for Cancer Research, National Cancer Institute, Frederick, Maryland 21702, United States

Ⓢ *Supporting Information*

**ABSTRACT:** Antiangiogenic agents (AA) are cytostatic, and their utility in cancer chemotherapy lies in their combination with cytotoxic chemotherapeutic agents. Clinical combinations of vascular endothelial growth factor receptor-2 (VEGFR2) inhibitors with antitubulin agents have been particularly successful. We have discovered a novel, potentially important analogue, that combines potent VEGFR2 inhibitory activity (comparable to that of sunitinib) with potent antitubulin activity (comparable to that of combretastatin A-4 (CA)) in a single molecule, with $GI_{50}$ values of $10^{-7}$ M across the entire NCI 60 tumor cell panel. It potently inhibited tubulin assembly and circumvented the most clinically relevant tumor resistance mechanisms (P-glycoprotein and $\beta$-III tubulin expression) to antimicrotubule agents. The compound is freely water-soluble as its HCl salt and afforded excellent antitumor activity *in vivo*, superior to docetaxel, sunitinib, or Temozolomide, without any toxicity.

**KEYWORDS:** *Antitubulin, antimitotic, antiangiogenic, VEGFR2 inhibition, combination chemotherapy*
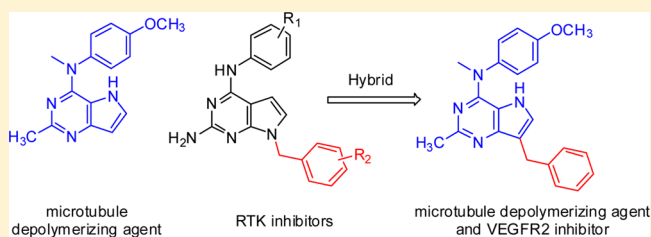
Antiangiogenic agents (AA) have defined a new paradigm for cancer treatment.[1] The principal mediator of angiogenesis is the vascular endothelial growth factor (VEGF) and its receptor tyrosine kinase (RTK) VEGFR2.[2] Rapid regrowth of vasculature in tumors after the removal of VEGFR2 inhibitors from the treatment regimen attests to their cytostatic mechanism.[3] VEGFR2 inhibitors are known to cause regression of impaired tumor blood vessels but transiently normalize the surviving vessels, which have less leakiness and are more like normal blood vessels. Such treatment therefore can transiently increase blood flow in the surviving vasculature.[4] Administering a cytotoxic agent during this transient tumor vasculature normalization provides improved drug delivery to the tumor, dependent on the surviving vasculature. However, administering separate antiangiogenic and cytotoxic agents may miss the timing window. Single entities with both antiangiogenic and cytotoxic components should allow the cytotoxicity to be manifested even at low concentrations in the tumor as soon as the antiangiogenic effect and vasculature normalization occur. Hence, these agents might not need the cytotoxic component to be as potent as conventional cytotoxic drugs and as such could perhaps avoid or reduce dose-limiting toxicities associated with conventional chemotherapy. Additionally, such single agents could circumvent pharmacokinetic problems

of multiple agents, avoid drug–drug interactions, and be used at lower doses to minimize toxicities and tumor cell resistance.

It has been our long-standing interest to design single entities with multiple targets.[5−8] We chose inhibition of tubulin as the mechanism for the cytotoxic effect because antitubulin agents are some of the most effective drugs in cancer chemotherapy.[9] Additionally, evidence for the remarkable clinical success of VEGFR2 inhibitors in combination with antitubulin agents is abundant in the literature.[10] Structural similarities of antitubulin[11] agents and RTK inhibitors[12] previously reported from our laboratory provided the rationale to incorporate structural features of both antitubulin activity and RTK inhibitory activity in single molecules to explore the possibility of providing dual inhibitory activities in single compounds. We[11] previously reported the design, synthesis, and antitumor activity of pyrrolo[3,2-*d*]pyrimidine (**1**; Figure 1), which inhibits tubulin assembly. Substituted 7-benzyl pyrrolo[2,3-*d*]pyrimidines with general structure **2** (Figure 1) were reported as antiangiogenic, antimetastatic, and antitumor agents.[9] Substituents on the benzyl group and the location of the benzyl group dictate RTK
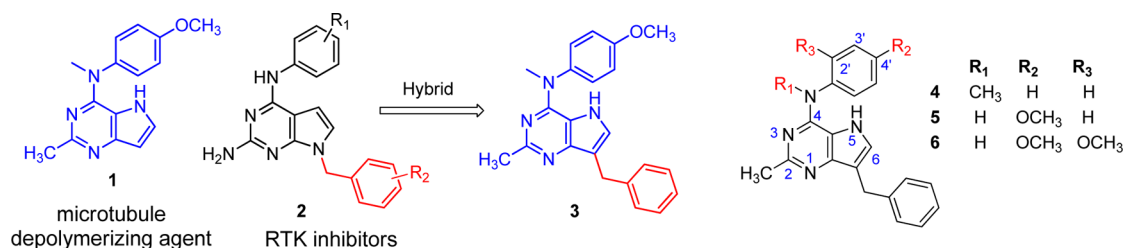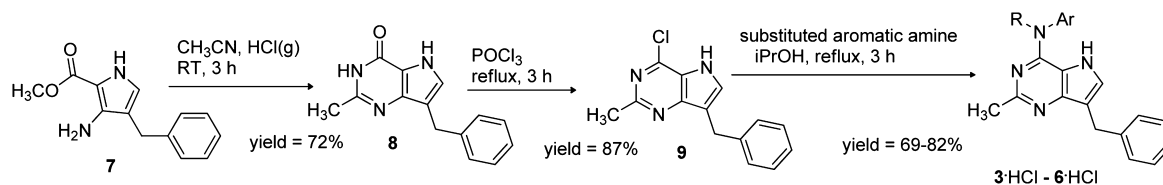
**Figure 1.** Hybrid design from lead compounds.



**Figure 2.** Synthesis of target compounds.

**Table 1. Inhibition of Tubulin Assembly and Cellular VEGFR2 Receptor Tyrosine Kinase and the Growth of $\beta$-III and P-gp Overexpressing Cells**

| compd | inhibition of tubulin assembly IC$_{50}$ ($\mu$M) | VEGFR2 inhibition IC$_{50}$ (nM) | WT HeLa IC$_{50}$ (nM) | $\beta$-III overexpressing HeLa IC$_{50}$ (nM) | parental OVCAR-8 IC$_{50}$ (nM) | P-gp overexpressing NCI/ADR-RES IC$_{50}$ (nM) |
|---|---|---|---|---|---|---|
| 1·HCl | 10 ± 0.6 | 182.3 ± 20.6 | nd | nd | nd | nd |
| 3·HCl | 21 ± 1 | 21.3 ± 3.2 | 280 ± 40 | 280 ± 40 | 1000 ± 300 | 700 ± 200 |
| 4·HCl | >20 (no act) | 50.1 ± 8.8 | >10,000 | >10,000 | | |
| 5·HCl | >20 (no act) | 40.6 ± 7.8 | >10,000 | >10,000 | | |
| 6·HCl | >40 (no act) | 30.1 ± 5.1 | | | >5,000 | >5,000 |
| CA | 1.2 ± 0.01 | | 1.8 ± 0.4 | 2.5 ± 0.7 | | |
| paclitaxel | | | 5.3 ± 2 | 16 ± 1 | 10 ± 0 | 5,000 ± 0 |
| semaxinib | | 12.9 | | | | |
| sunitinib | | 18.9 ± 2.7 | | | | |

inhibitory activity in pyrrolo[2,3-*d*]pyrimidines. Hence, having determined the antitubulin effects of **1**, it was of interest to engineer RTK inhibitory activity without loss of antitubulin activity by incorporating the 7-benzyl group onto the pyrrolo[3,2-*d*]pyrimidine scaffold. The results of this hybrid design afforded compound **3** (Figure 1). Compounds **4** and **5** were designed to evaluate the importance of the 4′-OCH$_3$ and the 4-NCH$_3$ moieties, respectively. Compound **6** was designed by incorporating a 2′-OCH$_3$ group to explore the effect of substituents at this position. The antimitotic activity of **3** also prompted its evaluation against cell lines which overexpress the multidrug resistance protein P-glycoprotein (Pgp) and the $\beta$-tubulin isoform $\beta$III. Tumors with either of these proteins are associated with significant resistance to antitubulin agents, especially with resistance to paclitaxel.[13]

**Chemistry.** Acid catalyzed condensation of pyrrole **7**[14] (Figure 2) with acetonitrile afforded bicyclic **8** in 72% yield. Next, **8** was chlorinated with POCl$_3$ to generate **9** in 87% yield. Compound **9** was subjected to nucleophilic displacement reactions using appropriately substituted aromatic amines to afford **3–6** in 69–82% yields.

*Inhibition of Tubulin Assembly.* Quantitative studies were conducted to determine the effects of these compounds on the polymerization of purified bovine brain tubulin. Compounds were compared with combretastatin A-4 (CA) as inhibitors of tubulin assembly (Table 1). Compound **3**·HCl was an effective *inhibitor of bovine tubulin assembly, albeit almost 18-fold less active than CA.*

*Inhibition of VEGFR2.* We chose to evaluate the VEGFR2 inhibitory activity of our compounds using human tumor cells known to express high levels of the VEGFR2. Compound **3**·HCl has inhibitory potency comparable with the clinically used sunitinib and clinically evaluated semaxinib against VEGFR2 (Table 1).

In order to rule out off target toxicity, we evaluated **3**·HCl with the assistance of a kinase profiling service (Luceome Biotechnologies)[15] against 48 other kinases (Supporting Information) and found no significant activity at 10 $\mu$M (data not shown).

**Structure−Activity Relationship.** The 7-benzyl moiety improved cellular VEGFR2 inhibition by about 9-fold and decreased inhibition of tubulin assembly by about 2-fold (comparing activities of **3**·HCl and lead compound **1**·HCl). The methyl group attached to the nitrogen bridge and the 4′-methoxy group were crucial for inhibition of tubulin (comparing activities of **5**·HCl and **4**·HCl with those of **3**·HCl). Removal of either of these groups resulted in complete loss of the ability to inhibit tubulin assembly and also decreased inhibition in VEGFR2 cellular activities.

**CAM Assay.** Compound **3**·HCl was tested for its effects on blood vessel formation in the chicken chorioallantoic membrane (CAM) antiangiogenic activity assay and was found to have an IC$_{50}$ value of 2.9 ± 0.32 $\mu$M comparable to sunitinib, IC$_{50}$ = 1.3 ± 0.07 $\mu$M.

*NCI 60 Tumor Panel.* (Table 2, Supporting Information). Compound **3**·HCl, showed a 3-digit nanomolar GI$_{50}$ in all the NCI 60 tumor cell lines, showing moderate cytotoxic activity
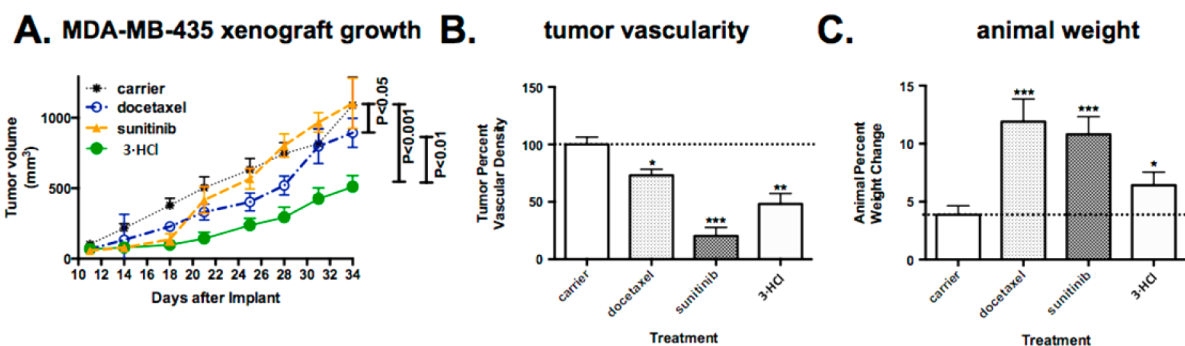
**Figure 3.** Treatment with **3**·HCl decreased primary tumor growth and tumor vascular density in the MDA-MB-435 flank xenograft model. *, $P < 0.05$; **, $P < 0.01$; ***, $P < 0.001$ by one way ANOVA with a Neuman−Keuls post-test. Human BLBCs, MDA-MB-435, were implanted into the lateral flank of NCr athymic nu/nu nude mice at 500,000 cells, and the mice were treated with carrier, docetaxel, sunitinib, or **3**·HCl twice weekly at their MTDs until the end of the experiment. Data is representative of 6−8 animals. (A) Tumor size was assessed by measuring tumor length, width, and depth twice weekly using Vernier calipers. Tumor volume was calculated with the ellipsoid formula: volume = 0.52 (length × width × depth) and graphically represented as days after implantation. Statistics on these graphs were two way ANOVA with repeated measures post-test. (B) Tumor vascular density was examined at the end of the experiment by staining tumor sections with CD31/PECAM-1 antibodies and a Vectastain ABC kit. Vascular density was determined by counting CD31-positive vessels and graphed as percent vessel density as compared with carrier treated animals. (C) Graphical representation of percent change in animal weight as determined by measuring animal weight at the beginning and end of the experiment.
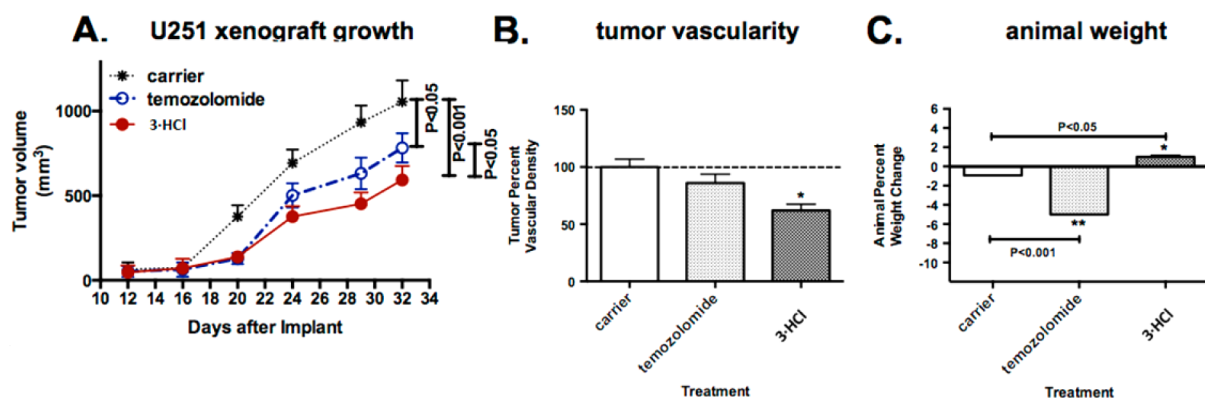


**Figure 4.** Treatment with **3**·HCl decreased primary tumor growth and tumor vascular density in a U251 flank xenograft mouse model. *, $P < 0.05$; **, $P < 0.01$; ***, $P < 0.001$ by one way ANOVA with a Neuman−Keuls post-test. U251 human glioma cells were implanted into the lateral flank of NCr athymic nu/nu nude mice at 500,000 cells, and the mice were treated with carrier Temozolomide or **3**·HCl twice weekly at their MTDs until the end of the experiment. Data is representative of 6−8 animals. (A) Tumor size was determined as described in the legend of Figure 3. Statistics on this graph were two way ANOVA with repeated measures post-test. (B) Tumor vascular density was examined at the end of the experiment as described in the legend of Figure 3. (C) Graphical representation of percent change in animal weight as determined by measuring animal weight at the beginning and end of the experiment.

(as desired) against tumor cells. The antiangiogenic component of **3**·HCl is not active in these cell culture assays.

*Effect on Pgp Overexpression and βIII-Tubulin Mediated Resistance to Paclitaxel.* The ability of **3**·HCl to overcome βIII-tubulin drug resistance was evaluated by using an isogenic HeLa cell line pair. While paclitaxel was 3-fold less potent in the βIII-tubulin overexpressing cell line than in the wild type HeLa cells, compound **3**·HCl inhibited both cell lines with equal potency without regard to their expression of βIII-tubulin.

The ability of **3**·HCl to circumvent Pgp-mediated drug resistance was evaluated by using an ovarian cancer cell line pair (Table 1). In this cell line pair, paclitaxel, which is a well-known Pgp substrate, was 500-fold less potent in the Pgp over-expressing cell line than in the wild type OVCAR-8 cells. Surprisingly, **3**·HCl is about 1.4-fold more potent in the Pgp overexpressing cell line. Hence, **3**·HCl is a poor substrate for transport by Pgp and thus has advantages over some clinically useful tubulin-targeting drugs such as paclitaxel, docetaxel, vinblastine, and vinorelbine.[13]

*Effects on Microtubules, Cell Cycle, and Apoptosis.* Tubulin staining in MDA-MB-435 cells and immunofluorescence imaging revealed that combretastatin A-4 phosphate (CA4P), a prodrug of CA converted to the active molecule probably by a phosphatase in the medium, and **3**·HCl led to less prominent and less aggregated microtubules as compared with control cells (Supporting Information), indicating that both compounds have similar effects on cellular microtubules.

Human MDA-MB-435 basal-like breast cancer cells (BLBCs)[16] were treated with an $IC_{50}$ dose of **3**·HCl, docetaxel, or CA4P and subjected to flow cytometric and cell cycle analysis. Analysis of DNA content and cell cycle determination showed an increase in the $G_2$/M phase of cells treated with **3**·HCl, as was the case with the antitubulin agents docetaxel and CA4P (Supporting Information), indicating that all three compounds arrest cells in mitosis, as is known for docetaxel and CA4P. Western blot analysis showed that **3**·HCl induced levels of the apoptosis markers, cleaved PARP, and cleaved caspase 3 (Supporting Information) after 48 h of treatment.
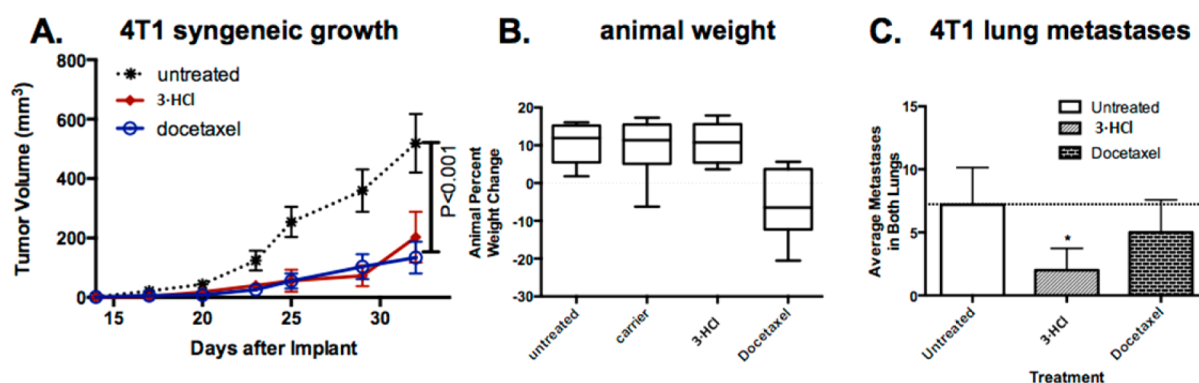
**Figure 5.** Treatment with **3**·HCl decreased primary tumor growth and lung metastases in the 4T1 orthotopic breast model. *, $P < 0.05$ by one way ANOVA with a Neuman−Keuls post-test. 4T1-Lucerase/GFP tagged cells were implanted orthotopically into BALB/c mice at 7500 cells, and the mice were treated with carrier, docetaxel, or **3**·HCl at their MTDs twice weekly until the end of the experiment. (A) Tumor volume was as described in the legend of Figure 3. (B) Animal weights were recorded before each treatment and graphed as percent weight change. (C) After 32 days, animals were euthanized and lungs were excised and immediately imaged at 25× using the LumaScope fluorescent imaging system. The number of metastases in both lungs was counted visually and represented graphically.

Taken together, these data show that **3**·HCl interferes with cellular microtubules, arrests cells in mitosis, and induces apoptosis.

**Identification of Binding Site on Tubulin.** Compound **3**·HCl failed to inhibit [3H]vinblastine binding to tubulin and nucleotide exchange, as measured by [8-14C]GTP binding to tubulin (Supporting Information). However, it inhibited [3H]colchicine binding by 55% ($\pm$2) at a concentration of 50 $\mu$M, indicating that **3**·HCl is probably a colchicine site-binding antitubulin agent.

*In Vivo Efficacy and Toxicity of **3**·HCl in Two Flank Tumor Models.* First, the maximal tolerated dose (MTD) of **3**·HCl, docetaxel, sunitinib, and Temozolomide was determined in mice (Supporting Information) and was used to examine the efficacy of **3**·HCl as compared with the antimicrotubule agent docetaxel and the VEGFR-2 inhibitor sunitinib on tumor growth in a flank xenograft mouse model *in vivo*. When MDA-MB-435 cancer cells were implanted into the flank of athymic mice, **3**·HCl significantly decreased the growth of primary tumors, both as compared with carrier treated mice and as compared with mice treated with docetaxel or with sunitinib (Figure 3A). Further, **3**·HCl decreased tumor vascular density (as measured by CD31/PECAM-1 immunohistochemical staining) as compared with carrier-treated and docetaxel-treated mice. However, sunitinib (Figure 3B) was more effective than **3**·HCl in reducing tumor vascular density. Finally, all of the treated animals gained weight during the study, indicating a lack of gross systemic toxicity (Figure 3C) in this experiment.

We also examined the effect of treatment with **3**·HCl on a human U251 glioma model implanted in immunodeficient mice in comparison with the standard clinically used agent Temozolomide (Figure 4). Compound **3**·HCl decreased primary tumor growth and tumor vascular density as compared with carrier and with Temozolomide without overt toxicity to the animals.

*Effect of **3**·HCl on Primary Tumor Growth and Lung Metastasis in the 4T1 Orthotopic Breast Cancer Model in Vivo.* We next sought to determine the *in vivo* efficacy of **3**·HCl in a relevant triple negative breast cancer model where metastasis can be assessed. Because the human MDA-MB-231 triple negative model requires 10 million cells, Matrigel, and immune deficient animals to grow *in vivo* and because the MDA-MB-468 line only metastasizes to the liver (unlike the

human tumor), we chose the mouse 4T1 triple negative orthotopic allograft model. It was found that **3**·HCl was as active as docetaxel at reducing primary tumor growth in the 4T1 model (Figure 5A). Significantly, **3**·HCl reduced lung metastases in this model better than did docetaxel, a key concept because most cancer patients die of metastatic disease (Figure 5C). Finally, treatment with **3**·HCl did not result in as much weight loss as with docetaxel, indicating less systemic toxicity to the animals (Figure 5B).

In summary, we have reported the design, synthesis, and biological evaluation for an agent that was designed to have both cytotoxic and antiangiogenic effects. The antiangiogenic effect is mediated *via* VEGFR2 inhibition. The cytotoxic effect is mediated by tubulin inhibition and is independent of overexpression of Pgp and $\beta$III-tubulin. The compound caused cellular microtubule depolymerization, arrested cells in the $G_2$/M phase, and triggered apoptotic cell death. *In vivo*, this compound reduced tumor size and vascularity in two flank xenograft models (the BLBC MDA-MB-435 and U251 glioma models) and in a 4T1 triple negative breast orthotopic allograft model. In these *in vivo* models, the activity of **3**·HCl was superior to those of Temozolomide (U251), docetaxel, and sunitinib (MDA-MB-435 and 4T1) without overt toxicity to the animals.

## ■ ASSOCIATED CONTENT

**ⓢ Supporting Information**

Tumor cell inhibitory activity (NCI) $GI_{50}$ (nM) of **3**·HCl, and the Experimental Section. This material is available free of charge via the Internet at http://pubs.acs.org.

## ■ AUTHOR INFORMATION

**Corresponding Author**

*E-mail: gangjee@duq.edu. Fax: 412-396-5593.

**Notes**

The authors declare no competing financial interest.

483

dx.doi.org/10.1021/ml4004793 | ACS Med. Chem. Lett. 2014, 5, 480−484

## ■ ABBREVIATIONS

AA, antiangiogenic agents; VEGFR2, vascular endothelial growth factor receptor-2; RTK, receptor tyrosine kinase; Pgp, P-glycoprotein; CAM, chicken chorioallantoic membrane; CA4P, combretastatin A-4 phosphate; BLBCs, basal-like breast cancer cells

## ■ REFERENCES

(1) Young, R. J.; Reed, M. W. Anti-angiogenic therapy: Concept to clinic. *Microcirculation* **2012**, *19*, 115−25.

(2) Shibuya, M. Vascular endothelial growth factor and its receptor system: Physiological functions in angiogenesis and pathological roles in various diseases. *J. Biochem.* **2013**, *153*, 13−19.

(3) Bergers, G.; Hanahan, D. Modes of resistance to anti-angiogenic therapy. *Nat. Rev. Cancer* **2008**, *8*, 592−603.

(4) Jain, R. K. Normalizing tumor microenvironment to treat cancer: Bench to bedside to biomarkers. *J. Clin. Oncol.* **2013**, *31*, 2205−2218.

(5) Gangjee, A.; Zaware, N.; Raghavan, S.; Ihnat, M.; Shenoy, S.; Kisliuk, R. L. Single agents with designed combination chemotherapy potential: Synthesis and evaluation of substituted pyrimido[4,5-*b*]indoles as receptor tyrosine kinase and thymidylate synthase inhibitors and as antitumor agents. *J. Med. Chem.* **2010**, *53*, 1563−1578.

(6) Gangjee, A.; Zhao, Y.; Ihnat, M. A.; Thorpe, J. E.; Bailey-Downs, L. C.; Kisliuk, R. L. Novel tricyclic indeno[2,1-*d*]pyrimidines with dual antiangiogenic and cytotoxic activities as potent antitumor agents. *Bioorg. Med. Chem.* **2012**, *20*, 4217−4225.

(7) Gangjee, A.; Li, W.; Lin, L.; Zeng, Y.; Ihnat, M.; Warnke, L. A.; Green, D. W.; Cody, V.; Pace, J.; Queener, S. F. Design, synthesis, and X-ray crystal structures of 2,4-diaminofuro[2,3-*d*]pyrimidines as multireceptor tyrosine kinase and dihydrofolate reductase inhibitors. *Bioorg. Med. Chem.* **2009**, *17*, 7324−7336.

(8) Gangjee, A.; Zeng, Y.; Ihnat, M.; Warnke, L. A.; Green, D. W.; Kisliuk, R. L.; Lin, F.-T. Novel 5-substituted, 2,4-diaminofuro[2,3-*d*]pyrimidines as multireceptor tyrosine kinase and dihydrofolate reductase inhibitors with antiangiogenic and antitumor activity. *Bioorg. Med. Chem.* **2005**, *13*, 5475−5491.

(9) Dumontet, C.; Jordan, M. A. Microtubule-binding Agents: A dynamic field of cancer therapeutics. *Nat. Rev. Drug Discovery* **2010**, *9*, 790−803.

(10) www.clinicaltrials.gov.

(11) Gangjee, A.; Pavana, R. K.; Li, W.; Hamel, E.; Westbrook, C.; Mooberry, S. L. Novel water-soluble substituted pyrrolo[3,2-*d*]-pyrimidines: design, synthesis, and biological evaluation as antitubulin antitumor agents. *Pharm. Res.* **2012**, *29*, 3033−3039.

(12) Gangjee, A.; Zaware, N.; Raghavan, S.; Yang, J.; Thorpe, J. E.; Ihnat, M. A. N(4)-(3-Bromophenyl)-7-(substituted benzyl) pyrrolo-[2,3-*d*]pyrimidines as potent multiple receptor tyrosine kinase inhibitors: design, synthesis, and *in vivo* evaluation. *Bioorg. Med. Chem.* **2012**, *20*, 2444−2454.

(13) Ganguly, A.; Cabral, F. New insights into mechanisms of resistance to microtubule inhibitors. *Biochim. Biophys. Acta* **2011**, *1816*, 164−171.

(14) Elliott, A. J.; Morris, P. E.; Petty, S. L.; Williams, C. H. An improved synthesis of 7-substituted pyrrolo[3,2-*d*]pyrimidines. *J. Org. Chem.* **1997**, *62*, 8071−8075.

(15) Luceome Biotechnologies, 1775 S. Pantano Rd, Suite 100, Tucson, AZ 85710.

(16) Chambers, A. F. MDA-MB-435 and M14 cell lines: Identical but not M14 melanoma? *Cancer Res.* **2009**, *69*, 5292−5293.

**484**

dx.doi.org/10.1021/ml4004793 | *ACS Med. Chem. Lett.* 2014, 5, 480−484